Harnessing Nonequilibrium Open Quantum Physics

-Exploring New Frontiers in Open Quantum Systems-

Masahito Ueda

Department of Physics and Institute for Physics of Intelligence, The University of Tokyo
RIKEN Center for Emergent Matter Science

quantum trajectory in path integral

Quantum Opt. 1 (1989) 131–151. Printed in the UK

Probability-density-functional description of quantum photodetection processes

M Ueda
NTT Basic Research Laboratories, 3-9-11, Midori-cho, Musashino-Shi, Tokyo 180, Japan

Received 11 April 1989, in final form 22 June 1989

Abstract. A concept 'probability-density functional' combined with the path integral technique is shown to provide a new framework for quantum photodetection theory. It replaces the conventional picture of unitary evolution of the total density operator followed by von Neumann's projection postulate for the case in which the effects of nonunitary state reduction and continuous measurements must be taken into account. This paper shows that an expression of the probability-density functional which incorporates both these effects provides complete quantum-statistical information about photoelectron statistics. Simple procedures are given for calculating the ensemble average and generating the functional of a quantity distributed in time.

quantum trajectory

Quantum Opt. 1 (1989) 131–151. Printed in the UK

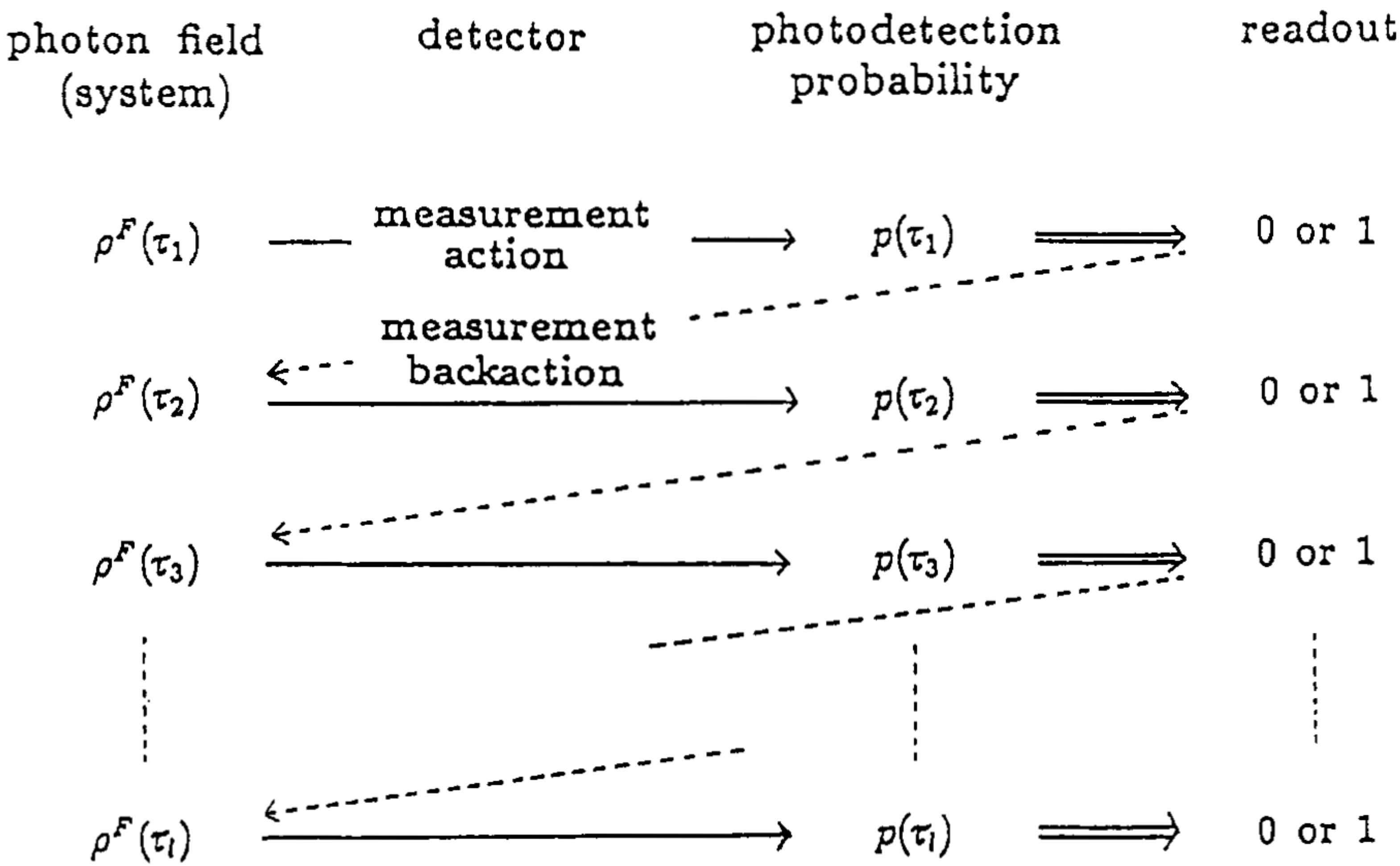

Figure 1. Nonunitary time evolution of photon statistics due to the real-time read-out of photoelectron statistics.

quantum trajectory

Quantum Opt. 1 (1989) 131–151. Printed in the UK

$$\mathcal{P}[p(c)] = \prod \exp\left(-\mathrm{i}\int p(t)u(t)\mathrm{d}t\right)\phi[u(c))]\delta\left(\frac{u(c)}{2\pi}\right)$$

path probability for continuous outcome c

unraveling

$$\rho(t+\tau) = T_\tau \rho(t) \qquad \rho(t) = \exp\left(\mathcal{L}t\right)\rho(0)$$

$$T_\tau = \sum_{m=0}^{\infty} \int_0^\tau \mathrm{d}t_m \int_0^{t_m} \mathrm{d}t_{m-1} \cdots \int_0^{t_2} \mathrm{d}t_1 \; S_{\tau-t_m}\, J\, S_{t_m - t_{m-1}} \cdots J\, S_{t_1}$$

$$J\rho(t) = \lambda a \rho(t) a^\dagger$$

one-photon process

$$S_\tau \rho(t) = \mathrm{e}^{-\mathrm{i}\omega a^\dagger a \tau}\, \rho(t) \mathrm{e}^{\mathrm{i}\omega a^\dagger a \tau}$$

no-photon process

Special thanks

Hongchao Li
U Tokyo

Xiehang Yu
MPI

Norifumi
Matsumoto
Fujitsu

Kohei
Kawabata
ISSP

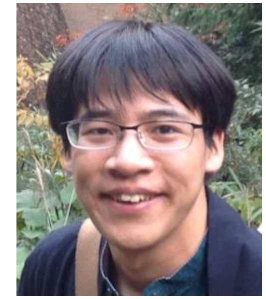

Ryusuke
Hamazaki
RIKEN

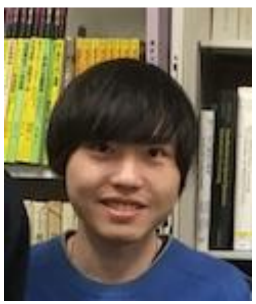

Zongping
Gong
U Tokyo

Sho
Higashikawa
Forcia

Yuto Ashida
U Tokyo

Masaya
Nakagawa
U Tokyo

Shunsuke
Furukawa
Keio

Naoto Tsuji, Kazuaki Takasan (U. Tokyo)
Ken Shiozaki, Masatoshi Sato (Kyoto U.)
Norio Kawakami (RIKEN), Kazuki Yamamoto (Osaka Metro. U)
Huixia Gao, Peng Xue (Beijing CSRC)

Why far-from-equilibrium physics important?

- Functionality emerges as we move away from equilibrium.
  (e.g., electronic devices, heat engines, biological systems)

- **Nonequilibrium quantum physics offer new research frontiers.**
  (e.g., dynamical topological phases, non-Hermitian physics)

dynamical topological phases: Floquet topological phases
topological pump
quantum channels, etc.

Why far-from-equilibrium physics important?

- Functionality emerges as we move away from equilibrium.
(e.g., electronic devices, heat engines, biological systems)

- Nonequilibrium quantum physics offer new research frontiers.
(e.g., dynamical topological phases, non-Hermitian physics)

- Growing needs for ever-faster information processing devices
(esp. advanced semiconductor devices, quantum computers)

Crucial question common to all of these is:
How can we create and stabilize nonequilibrium states?

Use of topological stability by using Maxwell's demon

M. Nakagawa and MU, Phys. Rev. X **15**, 021016 (2025)

Exploration of what's new in open quantum physics should start from revisiting the fundamental premise in closed quantum physics.

The most fundamental premise in closed quantum physics — Hermiticity

- **unitary dynamics**
- **real-valuedness of the eigenspectrum**
- **orthogonality of eigenstates**
- reciprocity ($\boldsymbol{O}^t$) = time reversal ($\boldsymbol{O}^*$)

- **"Open quantum" implies removal of one or more of these fundamental constraints.**
- **The key question:**
  What new potentials can be liberated therefrom?

Some ideas

- nonunitary dynamics & *PT*-symmetry
  → surpass the Lieb-Robinson bound
  PRL 120, 185301 (2018)

- complex eigenspectrum
  → intermediate-state eng., esp. magnetism reversal
  PRL 124, 147203 (2020)

- nonorthogonality of eigenstates
  → continuous QPT without gap closing
  PRL 125, 260601 (2020)

- reciprocity $(O^t) \neq$ time reversal (O^*)
  → unification and ramification of topological phases
  PRX 8, 031079 (2018)
  PRX 9, 041015 (2020)

$\boxed{10 \rightarrow 38}$

Some ideas

- **nonunitary dynamics & *PT*-symmetry**
  → surpass the Lieb-Robinson bound
  PRL 120, 185301 (2018)

- **complex eigenspectrum**
  → intermediate-state c ... etism reversal
  ...20)

- **nonortho ... enstates**
  → c ... without gap closing
  PRL 125, 260601 (2020)

- re ... city $(O^t) \neq$ time reversal (O^*)
  → unification and ramification of topological phases
  PRX 8, 031079 (2018)
  PRX 9, 041015 (2020)

$\boxed{10 \rightarrow 38}$

There are many undiscovered topological phases outside the Hermitian regime!

Nonunitary dynamics & *PT*-symmetry: surpassing the Lieb-Robinson bound

Y. Ashida and MU, Phys. Rev. Lett. **120**, 185301 (2018)

Solvable model: fermions under periodic dissipation

site-resolved detection of atom number

periodic dissipative potential (one-body loss)

half-filled free fermions in a superlattice

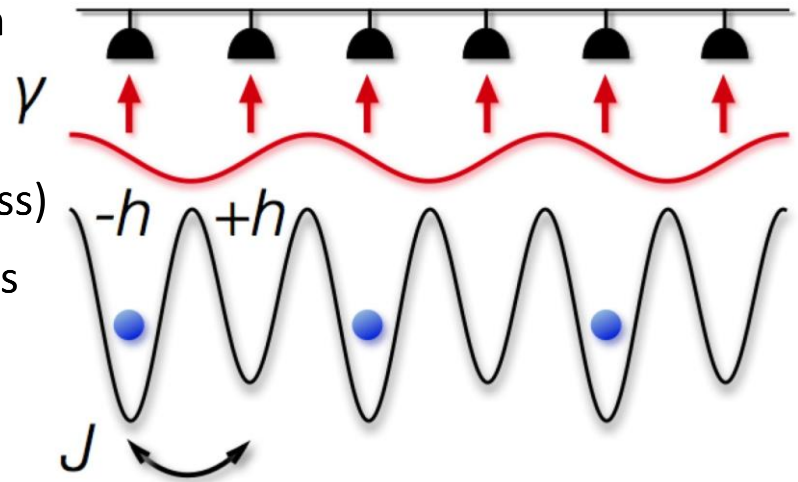

uniform one-body loss

effective Hamiltonian: $\hat{H}_{\mathrm{eff}} = \hat{H}_{\mathrm{PT}} - 2i\gamma\hat{N}$

***PT*-symmetric Hamiltonian:** $\hat{H}_{\mathrm{PT}} = -\sum_{l=0}^{L-1}\left[\left(J+(-1)^l i\gamma\right)\left(\hat{c}_{l+1}^\dagger\hat{c}_l+\hat{c}_l^\dagger\hat{c}_{l+1}\right)+(-1)^l h\hat{c}_l^\dagger\hat{c}_l\right]$

staggered on-site potential

quantum jump term: $\mathcal{J}[\hat{\rho}] = 2\gamma\sum_l[2\hat{c}_l\hat{\rho}\hat{c}_l^\dagger + (-1)^l(\hat{c}_l\hat{\rho}\hat{c}_{l+1}^\dagger + \hat{c}_{l+1}\hat{\rho}\hat{c}_l^\dagger)]$

Lindblad equation (ensemble level)

$$\frac{d\hat{\rho}(t)}{dt} = -i\left(\hat{H}_{\mathrm{eff}}\hat{\rho} - \hat{\rho}\hat{H}_{\mathrm{eff}}^\dagger\right) + \mathcal{J}[\hat{\rho}]$$

Y. Ashida and MU, PRL **120**, 185301 (2018)

Solvable model: fermions under periodic dissipation

site-resolved detection of atom number

periodic dissipative potential (one-body loss)

half-filled free fermions in a superlattice

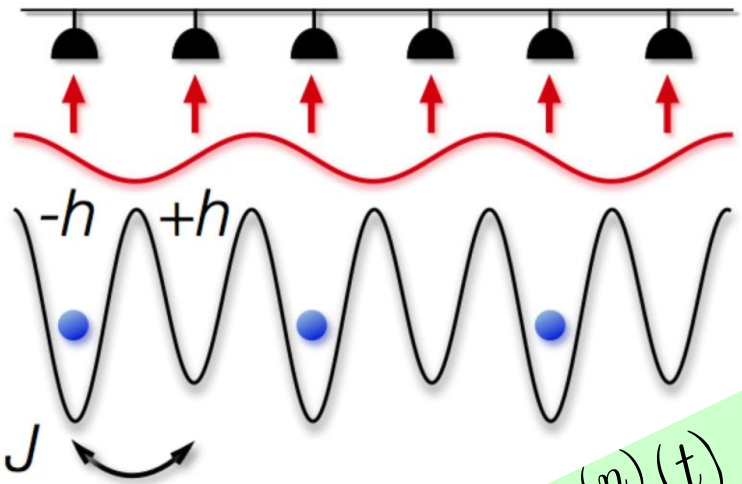

Exact solution for full-counting dynamics $\hat{\rho}^{(n)}(t)$ can be obtained!

…e-body loss

effective Hamiltonian: $\hat{H}_{\mathrm{eff}} = \hat{H}_{\mathrm{PT}} - 2i$ …

***PT*-symmetric Hamiltonian:** $\hat{H}_{\mathrm{P}}$ … $\sum_{l=0} \Big[\big(J + (-1)^l i\gamma\big)\Big(\hat{c}_{l+1}^\dagger \hat{c}_l + \hat{c}_l^\dagger \hat{c}_{l+1}\Big) + (-1)^l h \hat{c}_l^\dagger \hat{c}_l \Big]$

staggered on-site potential

quantum j… $\mathcal{J}[\hat{\rho}] = 2\gamma \sum_l [2\hat{c}_l \hat{\rho} \hat{c}_l^\dagger + (-1)^l (\hat{c}_l \hat{\rho} \hat{c}_{l+1}^\dagger + \hat{c}_{l+1} \hat{\rho} \hat{c}_l^\dagger)]$

Lindblad equation (ensemble level)

$$\frac{d\hat{\rho}(t)}{dt} = -i\left(\hat{H}_{\mathrm{eff}}\hat{\rho} - \hat{\rho}\hat{H}_{\mathrm{eff}}^\dagger\right) + \mathcal{J}[\hat{\rho}]$$

Y. Ashida and MU, PRL **120**, 185301 (2018)

Propagation of correlation: Lindblad dynamics

At t=0, we switch on dissipation γ and on-site potential h, and calculate the equal-time correlation function:

$$C(l,t)=\mathrm{Tr}[\hat{\rho}(t)\hat{c}_l^\dagger\hat{c}_0]$$

solution of Lindblad eq.

$$\hat{\rho}(t)=\sum_n P_n(t)\hat{\rho}^{(n)}(t)$$

Lieb-Robinson (LR) bound

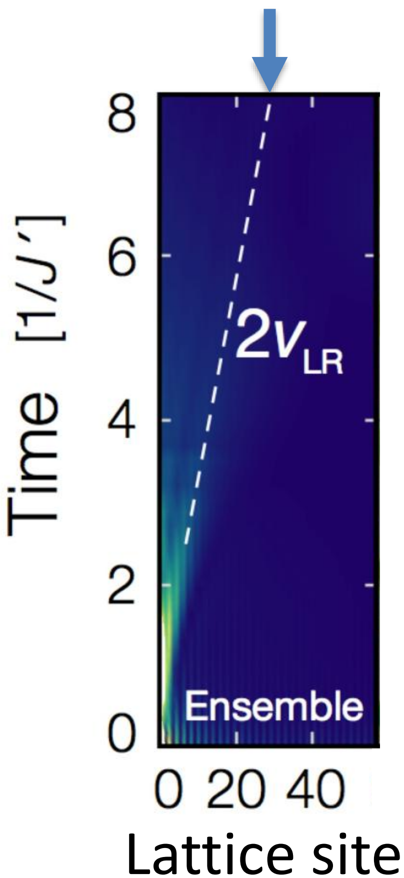

At the ensemble (i.e., Lindblad) level, the propagation of correlation is limited by the Lieb-Robinson bound.

cf. Poulin, PRL **104**, 190401 (2010)

Y. Ashida and MU, PRL **120**, 185301 (2018)

Propagation of correlation: full-counting dynamics

Same quantity under the full-counting dynamics for different numbers of quantum jumps *n*=0, 10, 20, 30, 40: $\hat{\rho}(t)=\sum_n P_n(t)\hat{\rho}^{(n)}(t)$

$$C^{(n)}(l,t)=\mathrm{Tr}[\hat{\rho}^{(n)}(t)\hat{c}_l^\dagger\hat{c}_0]$$

n: number of jumps

Faster propagation at integer multiples of LR bound!

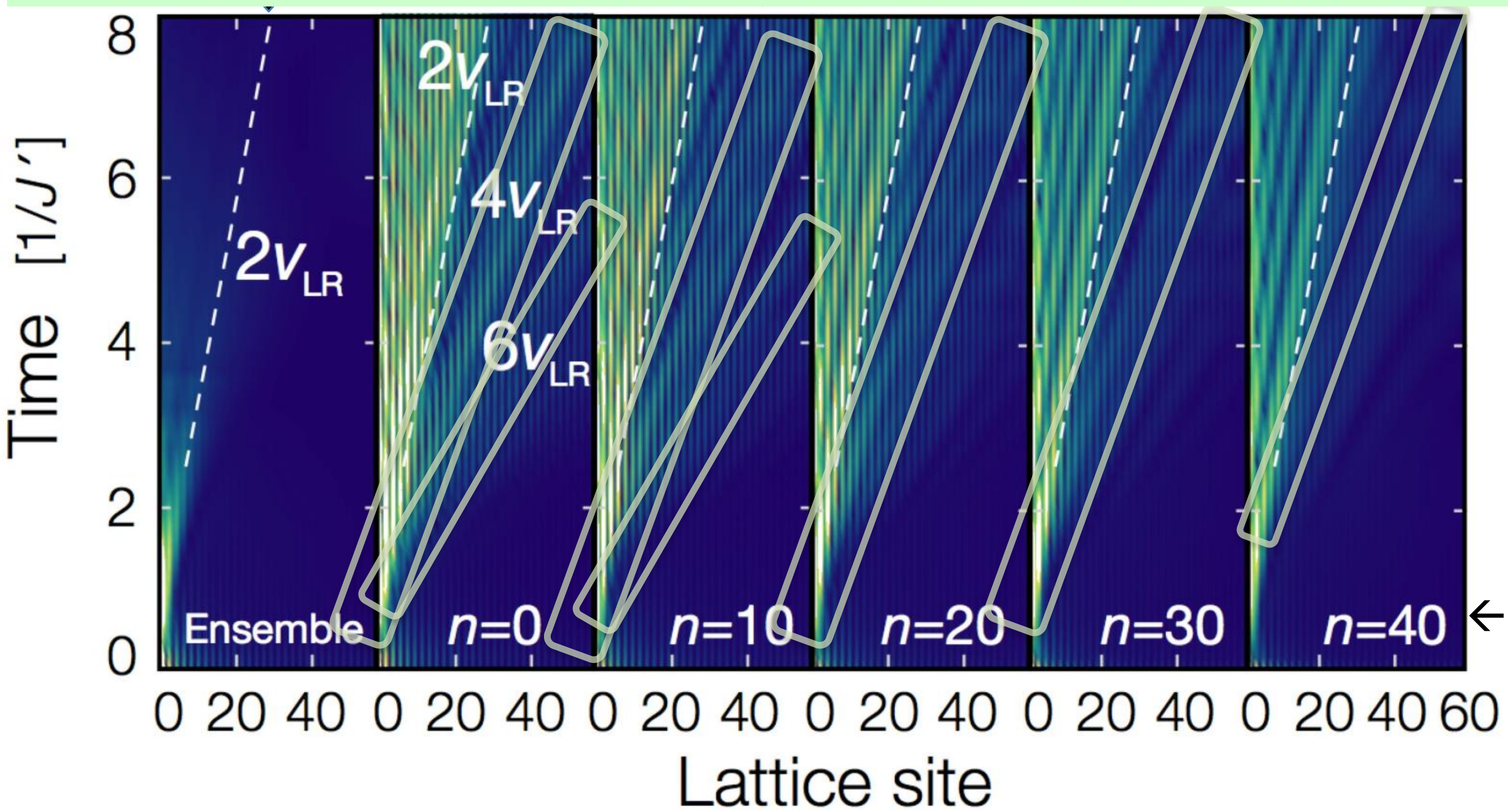

← **# of quantum jumps**

Y. Ashida and MU, PRL **120**, 185301 (2018)

Physical origin of supersonic propagation

PT-symmetric nonunitary dynamics

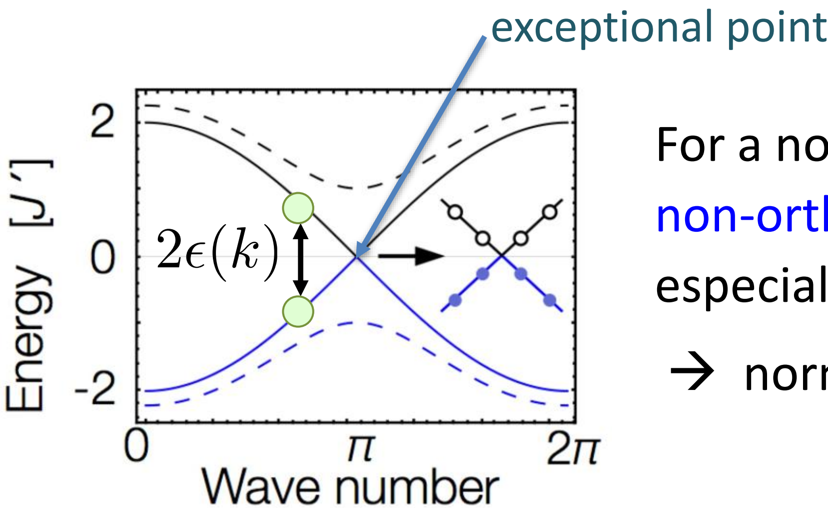

For a non-Hermitian system, eigenstates become non-orthogonal, mixing different eigenstates especially near the exceptional point.

→ norm oscillations at frequency $2\varepsilon(k)$.

Such higher harmonics modify the dispersion relation, leading to supersonic propagation.

$$v_{\mathrm{LR}} = \max_k \frac{\partial \epsilon(k)}{\partial(k/2)}$$

group velocity of quasiparticles

higher harmonics

$2\varepsilon(k)$, $4\varepsilon(k)$, …

→

supersonic propagation

$4v_{\mathrm{LR}}$, $6\, v_{\mathrm{LR}}$,…

Y. Ashida and MU, PRL **120**, 185301 (2018)

Complex eigenspectrum:

intermediate-state engineering & magnetism reversal

M. Nakagawa, et al., Phys. Rev. Lett. **124**, 147203 (2020)

Nontrivial many-body physics arises from higher-order processes in perturbation theory:

$$E_n^{(2)} = \sum_m{}' \frac{|V_{mn}|^2}{E_n^{(0)} - E_m^{(0)}}$$

Here an intermediate state plays a crucial role.

What happens if the intermediate energy has an imaginary part?

dissipative engineering of intermediate states

Magnetism can be reversed by dissipation.

Magnetism from spin-exchange interaction

Suppose that on-site interaction *U* >> hopping amplitude *t*.

◇ antiparallel spins → The system can lower energy via virtual hopping to the neighboring site.

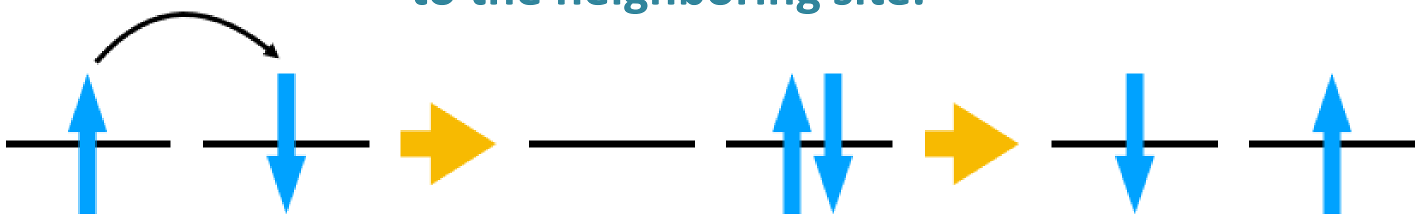

◇ parallel spins → The system cannot lower energy (Pauli principle).

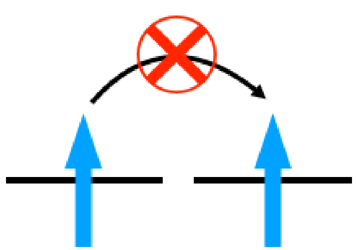

→ **antiferromagnetic Heisenberg model**

$$H = J \sum_{\langle i,j \rangle} \boldsymbol{S}_i \cdot \boldsymbol{S}_j \quad (J > 0)$$

Dissipative spin-exchange interaction

M. Nakagawa, et al., PRL **124**, 147203 (2020)

◇ antiparallel spins → The doubly occupied intermediate state decays due to inelastic collisions.

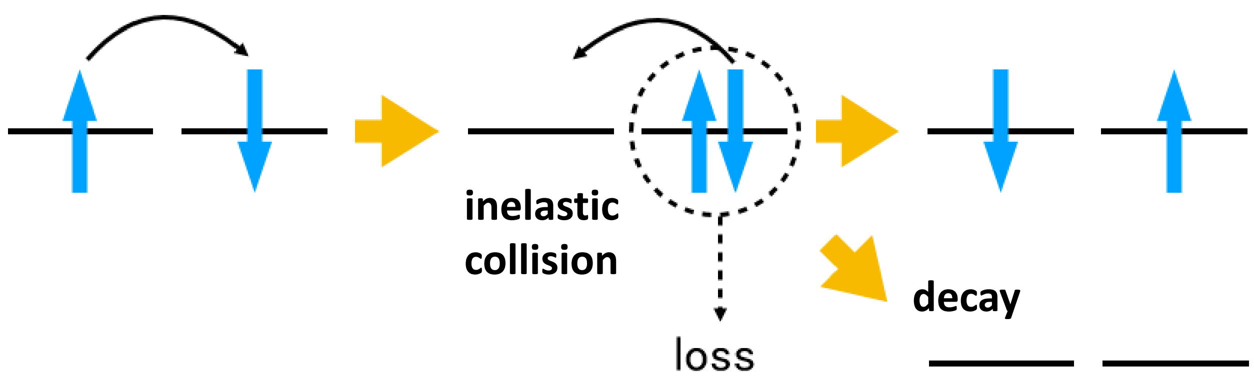

The antiferromagnetic interaction is suppressed by inelastic collisions.

Dissipative spin-exchange interaction

M. Nakagawa, et al., PRL **124**, 147203 (2020)

◇ antiparallel spins → The doubly occupied intermediate state decays due to inelastic collisions.

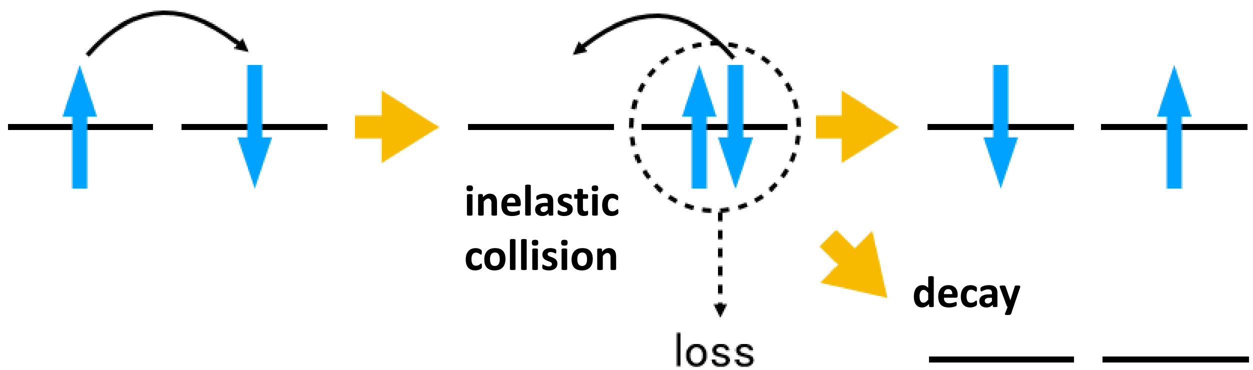

◇ parallel spins → The system is free from loss and stable.

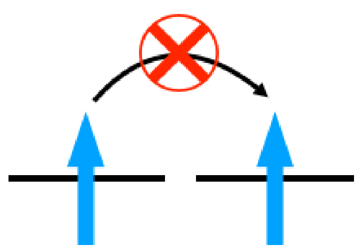

Higher-energy ferromagnetic states are stabilized by dissipation.

Dynamics of spin correlation of non-Hermitian Hubbard model

M. Nakagawa, et al., PRL **124**, 147203 (2020)

- **8 particles, 8 sites, $U/t = \gamma/t = 10$**

initial state = AFM Néel state |↑↓↑↓…>

$$C(i,j) = \langle\psi(\tau)|\,\boldsymbol{S}_i\cdot\boldsymbol{S}_j\,|\psi(\tau)\rangle\,/\,\langle\psi(\tau)|\psi(\tau)\rangle$$

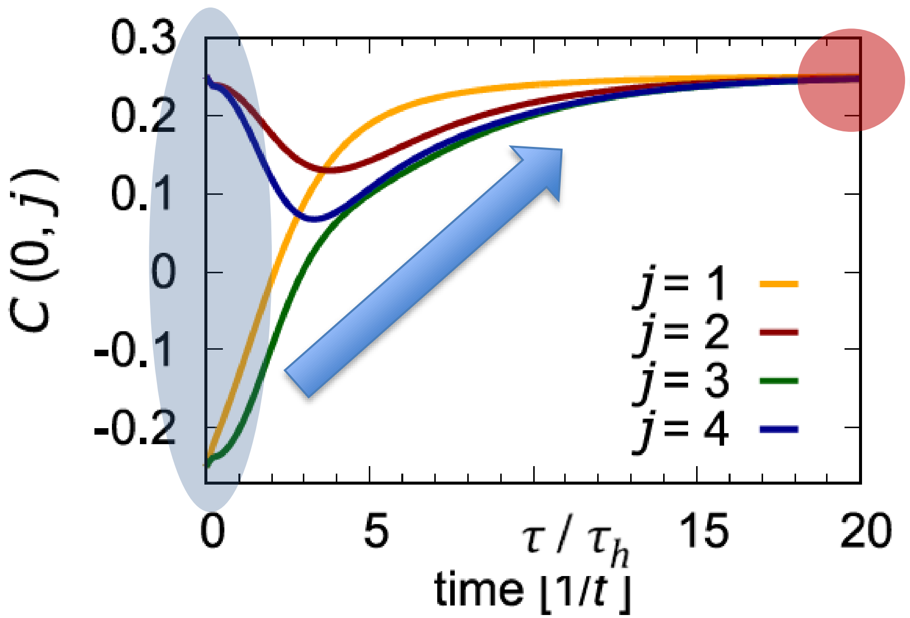

C (0, j) = 0.25 for all j

perfect ferromagnetism

Magnetism is inverted by dissipation.

Experimentally confirmed by the Kyoto group.

K. Honda, et al., PRL **130**, 063001 (2023)

Dissipative engineering of intermediate states

A similar idea should apply to other nontrivial many-body effects that arise from higher-order processes in perturbation theory:

$$E_n^{(2)} = \sum_m{}' \frac{|V_{mn}|^2}{E_n^{(0)} - E_m^{(0)}}$$

If we make the relevant intermediate-state energy complex, the lowest-energy state could become unstable and realize a previously unstable state.

Non-orthogonal eigenstates:

Continuous phase transition w/o gap closing

N. Matsumoto, et al., Phys. Rev. Lett. **125**, 260601 (2020)

In Hermitian systems, quantum phase transitions are accompanied by either

gap closing	**or**	**level crossing**
continuous QPT		**1^{st} order QPT**

The gap closing causes divergence in the fidelity susceptibility which is a signature of continuous QPT in Hermitian systems.

In non-Hermitian systems, non-orthogonality of eigenstates could make the fidelity susceptibility diverge without gap closing.

Fidelity susceptibility

$H(\lambda) = H_0 + \lambda V$ V causes a critical phenomenon.

$|\psi_n^R(\lambda)\rangle$ $(\langle\psi_n^L(\lambda)|)$ right (left) eigenstate with eigenenergy $E_n(\lambda)$

small variation of the coupling constant

$$F(\lambda, \delta\lambda) := \left|\langle\psi_0^R(\lambda)|\psi_0^R(\lambda + \delta\lambda)\rangle\right|$$

$$= 1 - \frac{1}{2}\delta\lambda^2 \underbrace{\sum_{\boxed{m,n\neq 0}} \frac{\langle\psi_0^R|V^\dagger|\psi_m^L\rangle}{(E_0 - E_m)^*} \frac{\langle\psi_n^L|V|\psi_0^R\rangle}{E_0 - E_n} \left(\langle\psi_m^R|\psi_n^R\rangle - \langle\psi_m^R|\psi_0^R\rangle\langle\psi_0^R|\psi_n^R\rangle\right)}_{\text{fidelity susceptibility } \chi_F(\lambda)}$$

Fidelity susceptibility

$H(\lambda) = H_0 + \lambda V$ V causes a critical phenomenon.

$|\psi_n^R(\lambda)\rangle$ $(\langle\psi_n^L(\lambda)|)$ right (left) eigenstate with eigenenergy $E_n(\lambda)$

$$F(\lambda, \delta\lambda) := \left|\langle\psi_0^R(\lambda)|\psi_0^R(\lambda+\delta\lambda)\rangle\right|$$

$$= 1 - \frac{1}{2}\delta\lambda^2 \underbrace{\sum_{\boxed{m,n\neq 0}} \frac{\langle\psi_0^R|V^\dagger|\psi_m^L\rangle}{(E_0 - E_m)^*} \frac{\langle\psi_n^L|V|\psi_0^R\rangle}{E_0 - E_n} \left(\langle\psi_m^R|\psi_n^R\rangle - \langle\psi_m^R|\psi_0^R\rangle\langle\psi_0^R|\psi_n^R\rangle\right)}_{\text{fidelity susceptibility } \chi_F(\lambda)}$$

For a Hermitian system, this double sum reduces to a single sum due to the orthogonality of eigenstates:

$$\chi_F(\lambda) = \sum_{\boxed{n}}{}' \frac{|\langle\psi_n(\lambda)|V|\psi_0(\lambda)\rangle|^2}{|E_0(\lambda) - E_n(\lambda)|^2}$$

divergence ↔ gap closes

single sum

Nonorthogonality-Induced Divergence

$$F(\lambda, \delta\lambda) := \left| \left\langle \psi_0^R(\lambda) \middle| \psi_0^R(\lambda + \delta\lambda) \right\rangle \right|$$

$$= 1 - \frac{1}{2}\delta\lambda^2 \underbrace{\sum_{\boxed{m,n\neq 0}} \frac{\langle \psi_0^R | V^\dagger | \psi_m^L \rangle}{(E_0 - E_m)^*} \frac{\langle \psi_n^L | V | \psi_0^R \rangle}{E_0 - E_n} \left(\langle \psi_m^R | \psi_n^R \rangle - \langle \psi_m^R | \psi_0^R \rangle \langle \psi_0^R | \psi_n^R \rangle \right)}_{\text{fidelity susceptibility } \chi_F(\lambda)}$$

However, for non-Hermitian systems, eigenstates are not orthogonal to each other.

The double sum can cause divergence without gap closing.

Non-Hermitian Toric-Code Model

N. Matsumoto et al., PRL **125**, 260601 (2020)

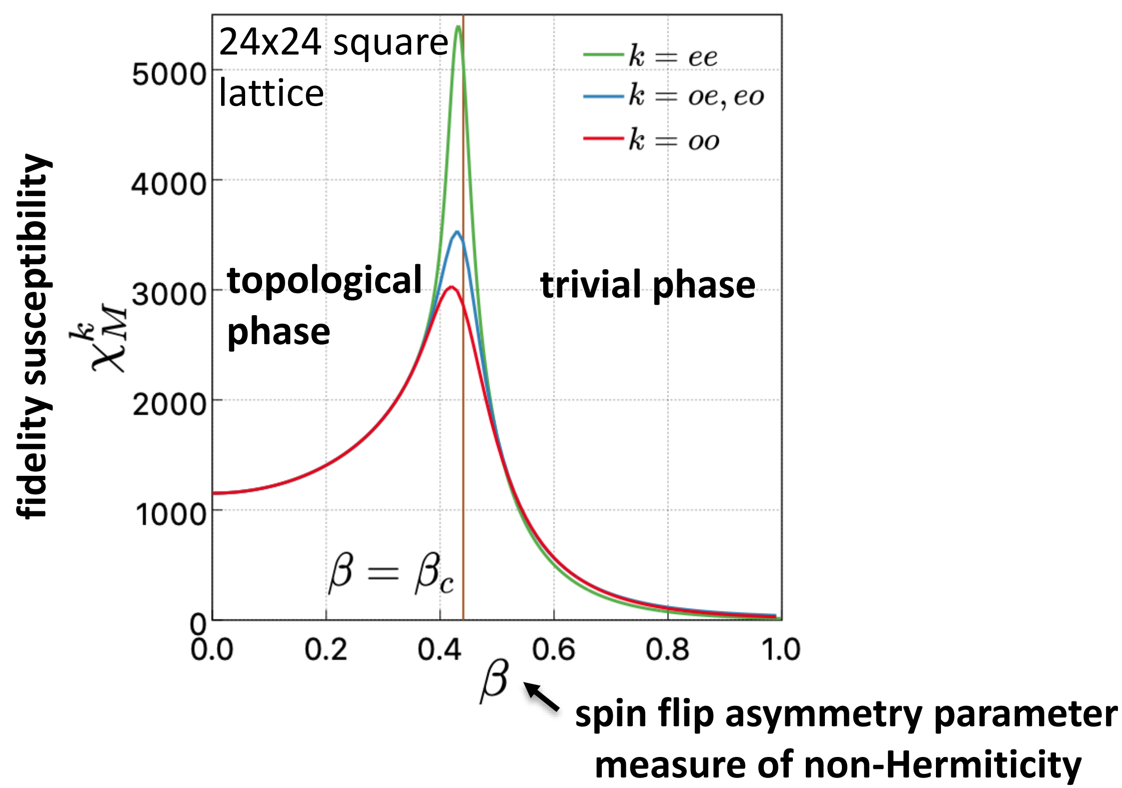

Non-Hermitian Toric-Code Model

N. Matsumoto et al., PRL **125**, 260601 (2020)

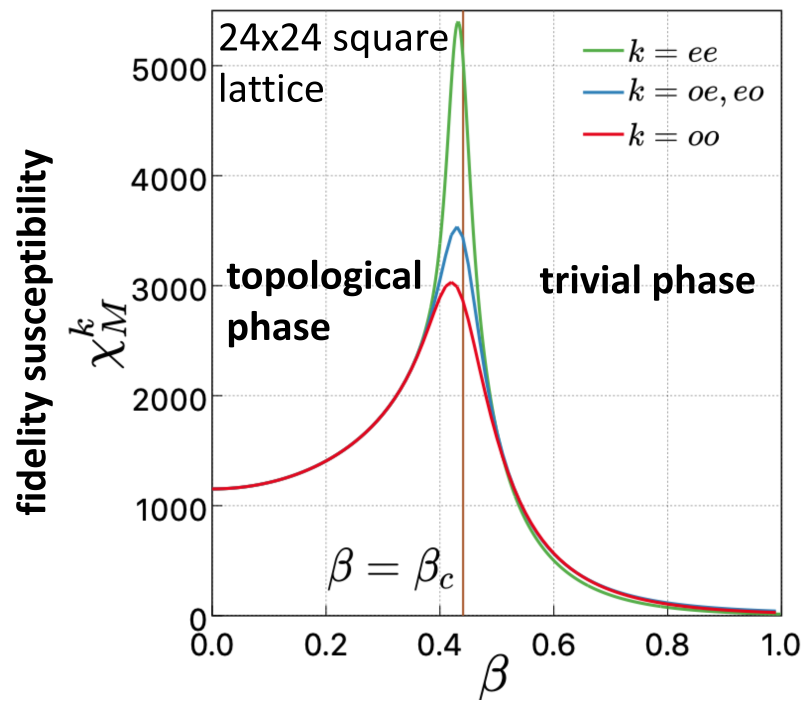

In this model, there is no gap closing as β changes.
Yet, the fidelity susceptibility diverges at the transition point between topological and trivial phases.

Two sides of the same coin

- **Fidelity susceptibility** $\sim \frac{\hbar v_{LR}}{\Delta}$

- **Its divergence means that either Δ vanishes or** v_{LR} **diverges.**

- **Δ=0 → Hermitian**
  $v_{LR} = \infty$ **→ non-Hermitian**

Beyond-hermiticity implies expansion of topological phases: 10 → 38

Three key features of Hermiticity

- Hermiticity ensures the equivalence between $H^T = H^*$.

  reciprocity (H^T) = time reversal (H^*)

- Hermiticity ensures the equivalence between $H^\dagger = H$.

  chiral sym ($\Gamma H^\dagger \Gamma^{-1} = -H$) = sublattice sym ($\Gamma H \Gamma^{-1} = -H$)

- **Hermiticity ensures real-valuedness of the eigenspectrum.**

  There is only one type of energy gap.

Complex energy spectra → two types of energy gaps

K. Kawabata *et al.*, PRX **9**, 041015 (2019)

Point gap

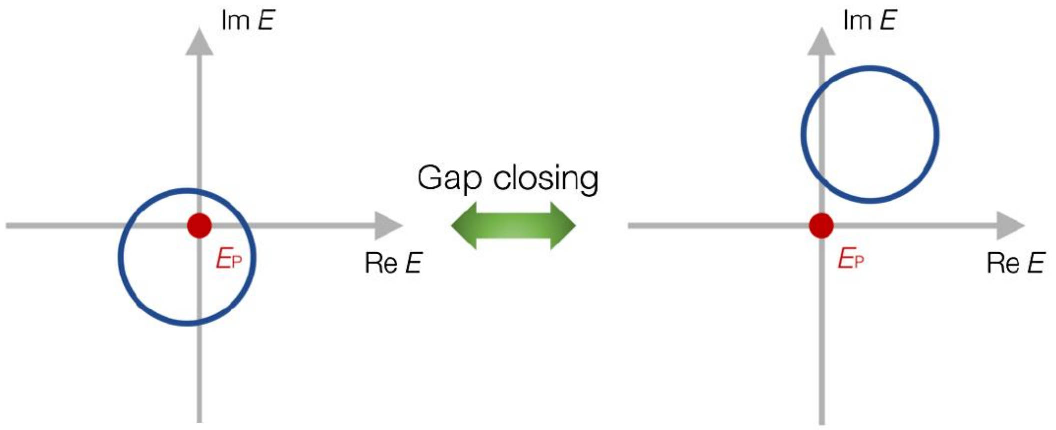

Line gap

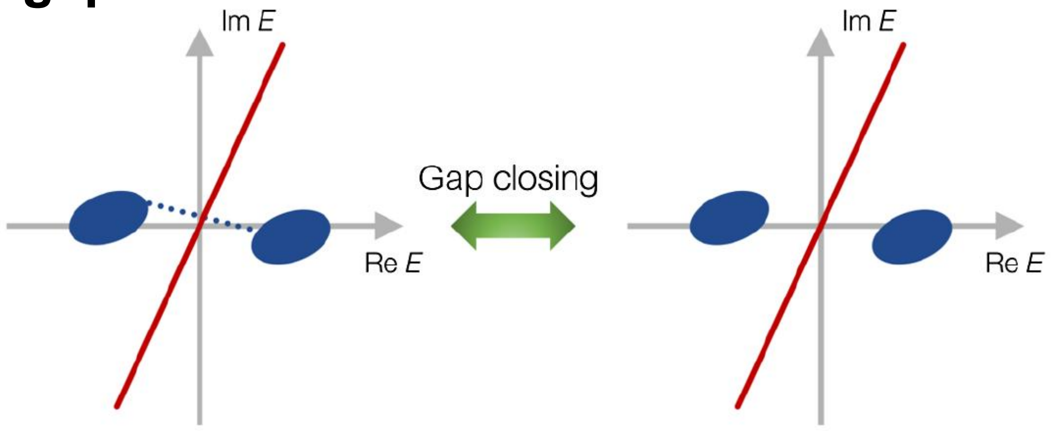

If we remove hermitian constraints, we can achieve topological unification and ramification.

K. Kawabata *et al.*, Nat. Commun. **10**, 297 (2019)

non-Hermitian symmetry classes
10 (Hermitian)→ 38 (non-Hermitian)

K. Kawabata, *et al*., PRX **9**, 041015 (2019)

H. Zhou and J. Y. Lee, PRB **99**, 235112 (2019)

Y. Ashida*, et al*., Adv. Phys. **69**, 249 (2020)

Exploring New Physics Frontiers

- Statistical physics
- Condensed matter physics
- Cold atoms

Quantum simulation of statistical physics:

Yang-Lee zeros & nonunitary criticality

What's Yang-Lee Zeros?

C. N. Yang & T. D. Lee, Phys. Rev. **87**, 404 (1952)
T. D. Lee & C. N. Yang, Phys. Rev. **87**, 410 (1952)

Yang-Lee zeros = zeros of the partition function

However, the partition function vanishes only when some physical parameters, such as *B* and *T*, are made complex.

This is definitely unphysical. But, analytic properties of the partition function can be found from the distribution of zeros.

Yang and Lee used this fact to investigate fundamental properties of phase transitions.

Yang-Lee Zeros and Edge Singularity

Zeros of the grand partition function of the Ising model are distributed on a **unit circle** **of a complex fugacity** ***z*****=exp(-2βH).**

C. N. Yang & T. D. Lee, Phys. Rev. **87**, 404 (1952)
T. D. Lee & C. N. Yang, Phys. Rev. **87**, 410 (1952)

The partition function vanishes for pure imaginary magnetic fields.

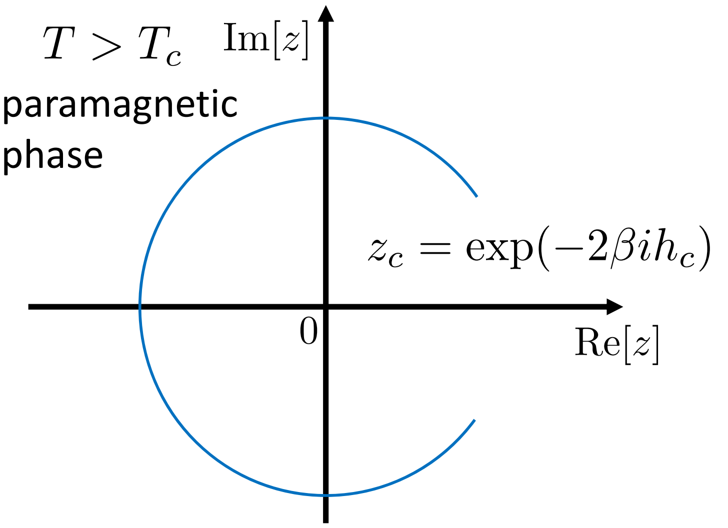

Yang-Lee Zeros and Edge Singularity

Yang and Lee proved that zeros of the grand partition function are distributed on a unit circle of a complex fugacity $z=\exp(-2\beta H)$.

C. N. Yang & T. D. Lee, Phys. Rev. **87**, 404 (1952)
T. D. Lee & C. N. Yang, Phys. Rev. **87**, 410 (1952)

Moreover, the edges of the distribution are shown to exhibit nonunitary critical phenomena known as the Yang-Lee edge singularity.

P. Kortman & R. Griffiths, PRL **27**, 1439 (1971)
M. Fisher, PRL **40**, 1610 (1978)

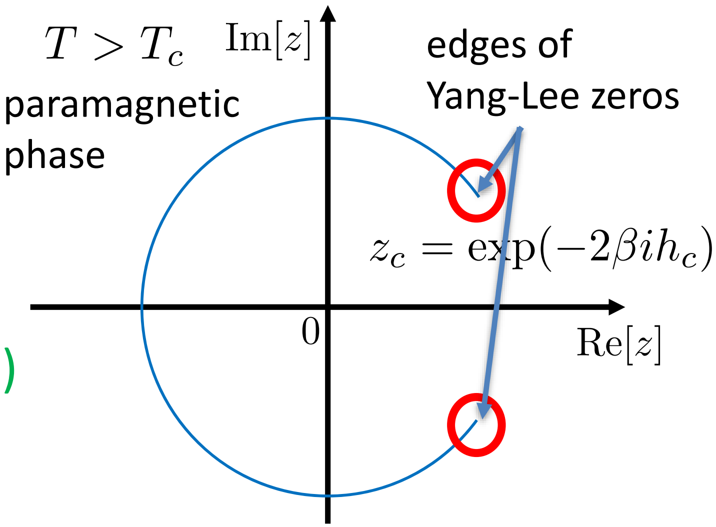

density of the distribution of Yang-Lee zeros near the edges

$$g(h) \propto (h - h_c)^{\sigma}$$

(critical exponent $\sigma < 1$)

However, since the Yang-Lee zeros appear for imaginary magnetic fields ($H=\pm ih$), physical implementation of Yang-Lee zeros is highly nontrivial.

Our idea
To map the model to a *PT*-symmetric one

N. Matsumoto *et al*., Phys. Rev. Res. **4**, 033250 (2022)

Mapping

Lee and Yang considered the classical one-dimensional Ising model under an imaginary magnetic field:

$$H = -J \sum_j \sigma_j \sigma_{j+1} - ih \sum_j \sigma_j$$

This classical system can be mapped via the quantum-classical correspondence to a zero-dimensional *PT*-symmetric qubit Hamiltonian:

$$\boxed{\begin{aligned} &H_{\mathrm{PT}} = R(\cos\phi)\sigma^x + iR(\sin\phi)\sigma^z \\ &[H_{\mathrm{PT}}, \mathcal{PT}] = 0 \text{ with } \mathcal{P} = \sigma^x \text{ and } \mathcal{T} = \mathcal{K} \end{aligned}}$$

N. Matsumoto *et al*., Phys. Rev. Res. **4**, 033250 (2022)

Direct Observation of Yang-Lee Physics using Heralded Photons

H. Gao *et al.*, PRL **132**, 176601 (2024)

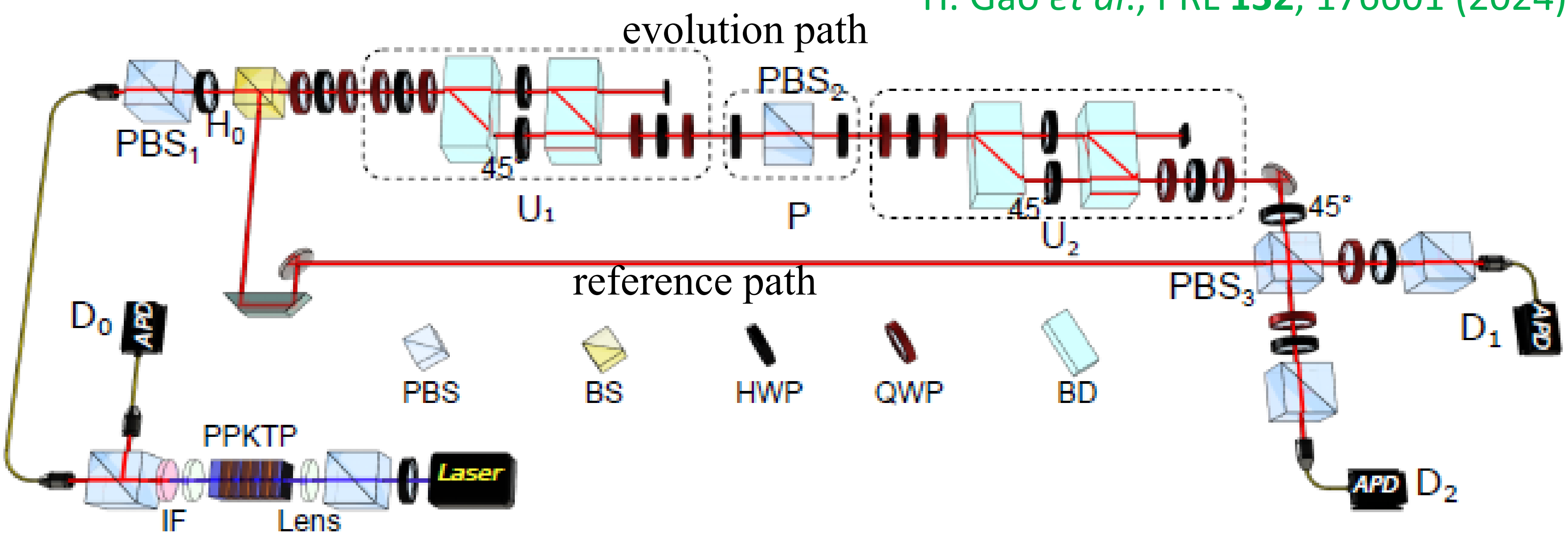

$$H_{\mathrm{PT}} = R(\cos\phi)\sigma^x + iR(\sin\phi)\sigma^z$$

This mapped *PT*-symmetric Hamiltonian can be implemented experimentally using heralded single photons.

Direct Observation of Yang-Lee Physics using Heralded Photons

H. Gao *et al.*, PRL **132**, 176601 (2024)

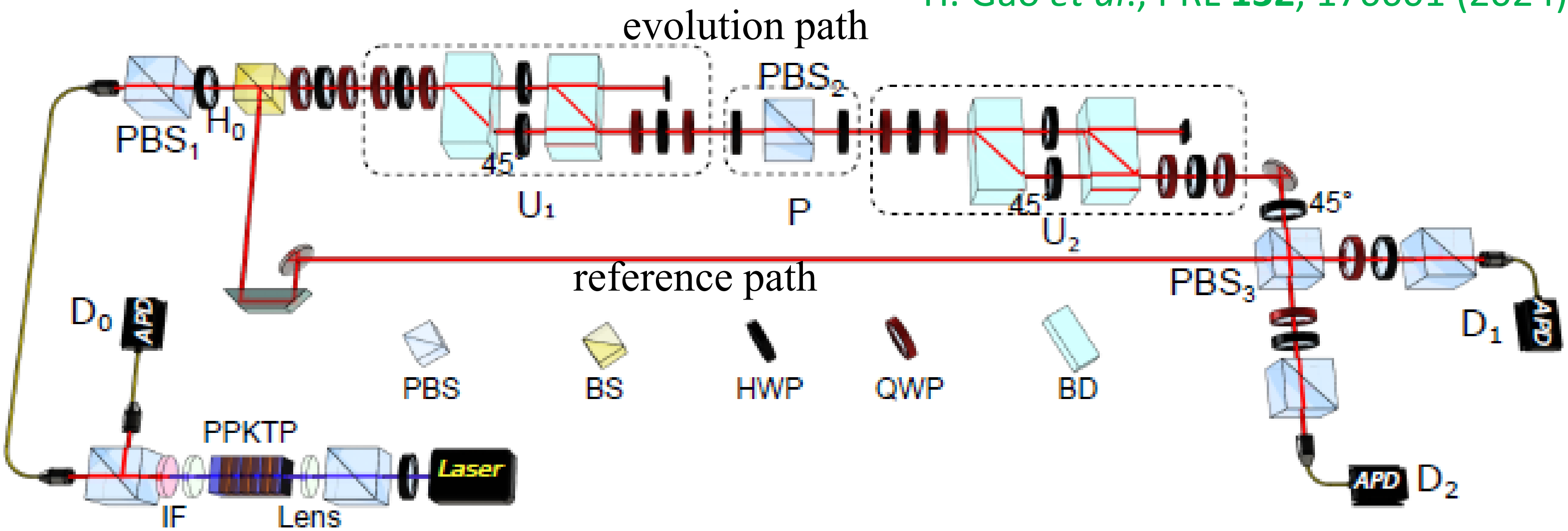

$$H_{\mathrm{PT}} = R(\cos\phi)\sigma^x + iR(\sin\phi)\sigma^z$$

The horizontal and vertical polarization states serve as basis states for a qubit system ($|0\rangle = |H\rangle$, $|1\rangle = |V\rangle$), and optical loss is fine-tuned to dynamically simulate the *PT*-symmetric system.

Decisive Advantage of Photonic Experiments

H. Gao *et al.*, PRL **132**, 176601 (2024)

Typical measurements yield 240,000 photons per second, ensuring sufficient statistical accuracy for testing critical phenomena.

Not just physical quantities such as magnetization *m*, but also the partition function *Z* can be measured directly.

$$m = \langle \sigma_z \rangle = \frac{\langle H| e^{-\beta H_{\mathcal{PT}}} |H\rangle - \langle V| e^{-\beta H_{\mathcal{PT}}} |V\rangle}{\langle H| e^{-\beta H_{\mathcal{PT}}} |H\rangle + \langle V| e^{-\beta H_{\mathcal{PT}}} |V\rangle}$$

$$Z = \langle H| e^{-\beta H_{\mathcal{PT}}} |H\rangle + \langle V| e^{-\beta H_{\mathcal{PT}}} |V\rangle \quad (t = -\mathrm{i}\,\beta)$$

Phase diagram

H. Gao *et al.*, PRL **132**, 176601 (2024)

$$H_{\mathrm{PT}} = R(\cos\phi)\sigma^x + iR(\sin\phi)\sigma^z$$

This photonic *PT*-symmetric Hamiltonian has two phases – *PT*-unbroken phase and *PT*-broken phase – intervened by the quantum critical point (QCP).

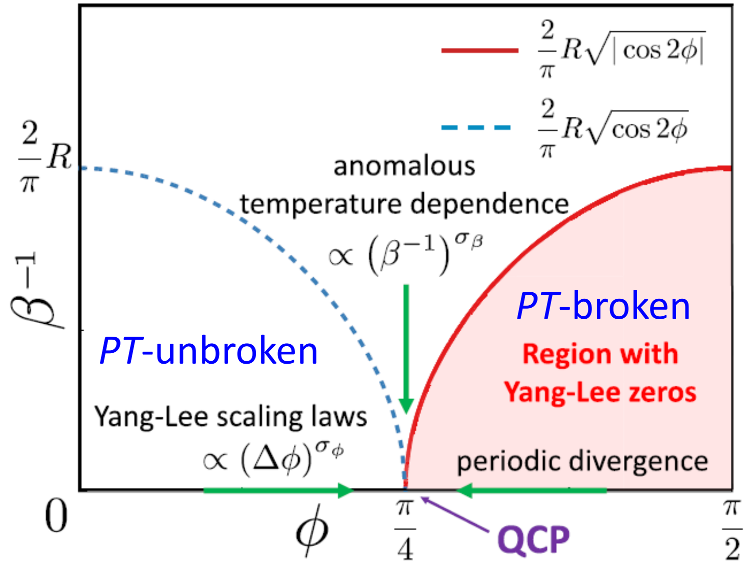

PT-unbroken phase: classical Yang-Lee scaling

H. Gao *et al.*, PRL **132**, 176601 (2024)

In the *PT*-unbroken phase, *m* and χ should show scaling laws consistent with the classical Yang-Lee scaling laws:

$$m \to \frac{-i\sin\phi}{\sqrt{\cos 2\phi}} \propto \Delta\phi^{-\frac{1}{2}}, \qquad \chi \to \frac{-i\cos^3\phi}{\cos^{\frac{3}{2}} 2\phi} \propto \Delta\phi^{-\frac{3}{2}}$$

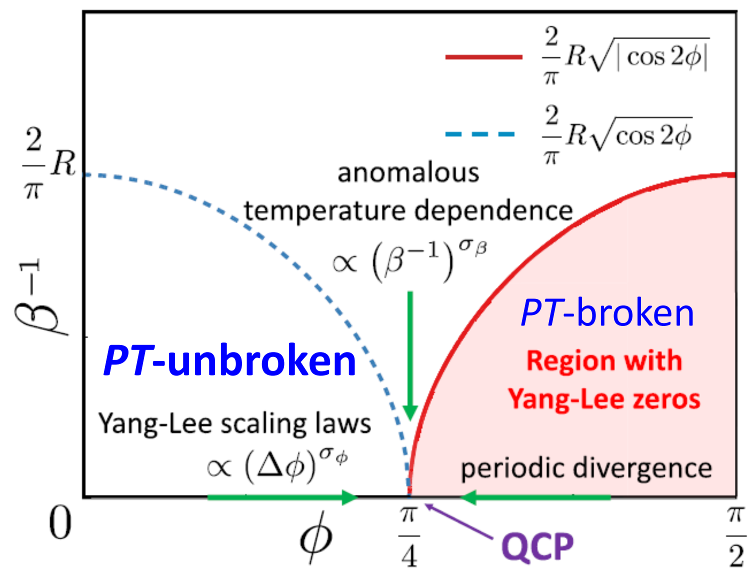

PT-unbroken phase: classical Yang-Lee scaling

H. Gao *et al.*, PRL **132**, 176601 (2024)

In the *PT*-unbroken phase, *m* and χ should show scaling laws consistent with the classical Yang-Lee scaling laws:

$$m \to \frac{-i\sin\phi}{\sqrt{\cos 2\phi}} \propto \Delta\phi^{-\frac{1}{2}}, \qquad \chi \to \frac{-i\cos^3\phi}{\cos^{\frac{3}{2}} 2\phi} \propto \Delta\phi^{-\frac{3}{2}}$$

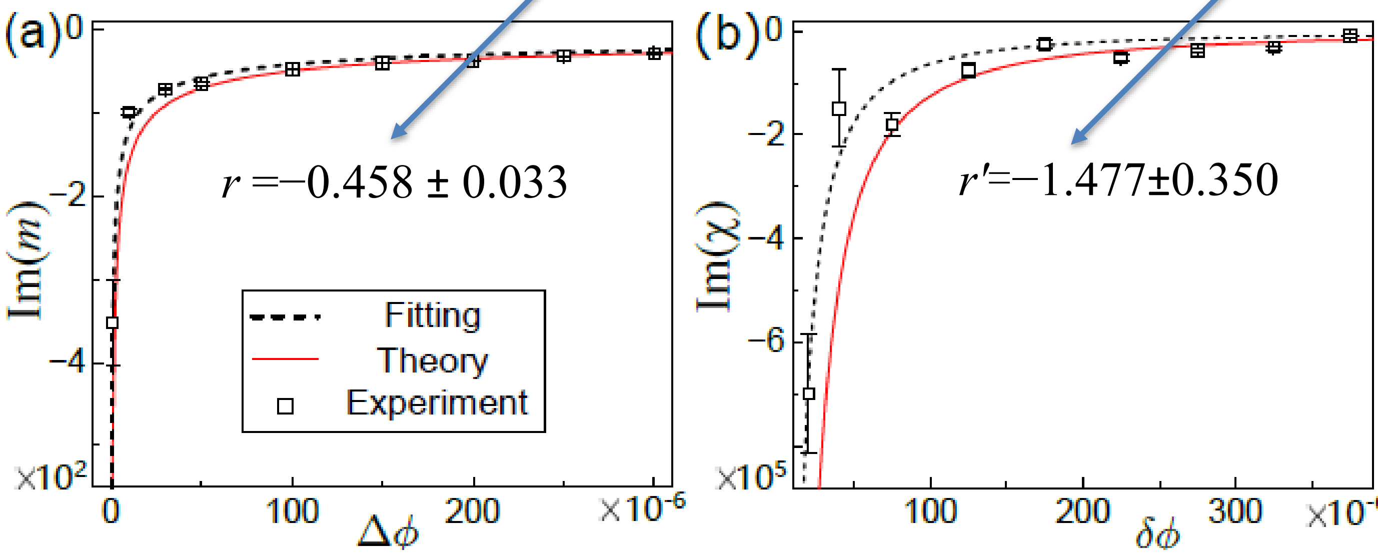

The measured results are consistent with theoretical predictions.

At the *PT* transition point: anomalous scaling

H. Gao *et al.*, PRL **132**, 176601 (2024)

At the *PT* transition point ($\phi=\pi/4$), *m* and χ show anomalous scaling with negative critical exponents (-1 and -3):

$$m \to -\frac{i}{\sqrt{2}}\beta R, \quad \chi \to -\frac{i}{3\sqrt{2}}\left(\beta^3 R^3 + \frac{3}{2}\beta R\right) \quad t = -i\beta$$

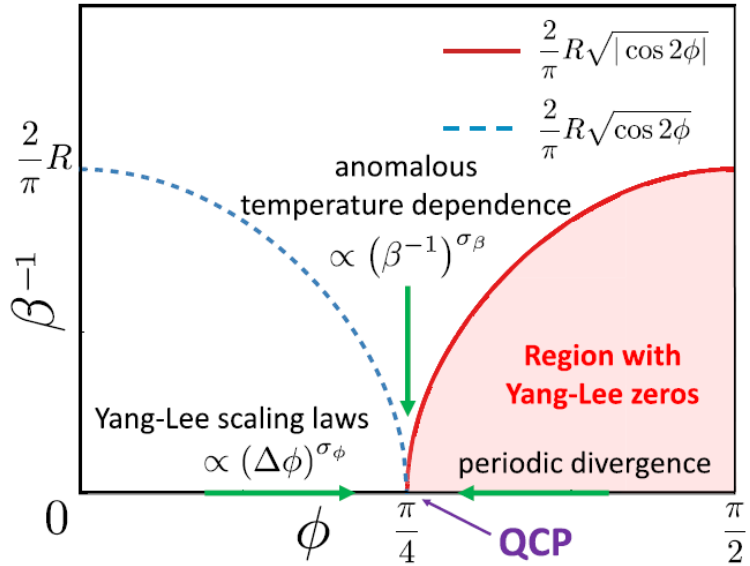

At the *PT* transition point: anomalous scaling

H. Gao *et al.*, PRL **132**, 176601 (2024)

At the *PT* transition point (ϕ=π/4), *m* and *χ* show anomalous scaling with negative critical exponents (-1 and -3):

$$m \to -\frac{i}{\sqrt{2}}\beta R, \quad \chi \to -\frac{i}{3\sqrt{2}}(\beta^3 R^3 + \frac{3}{2}\beta R) \quad t = -i\beta$$

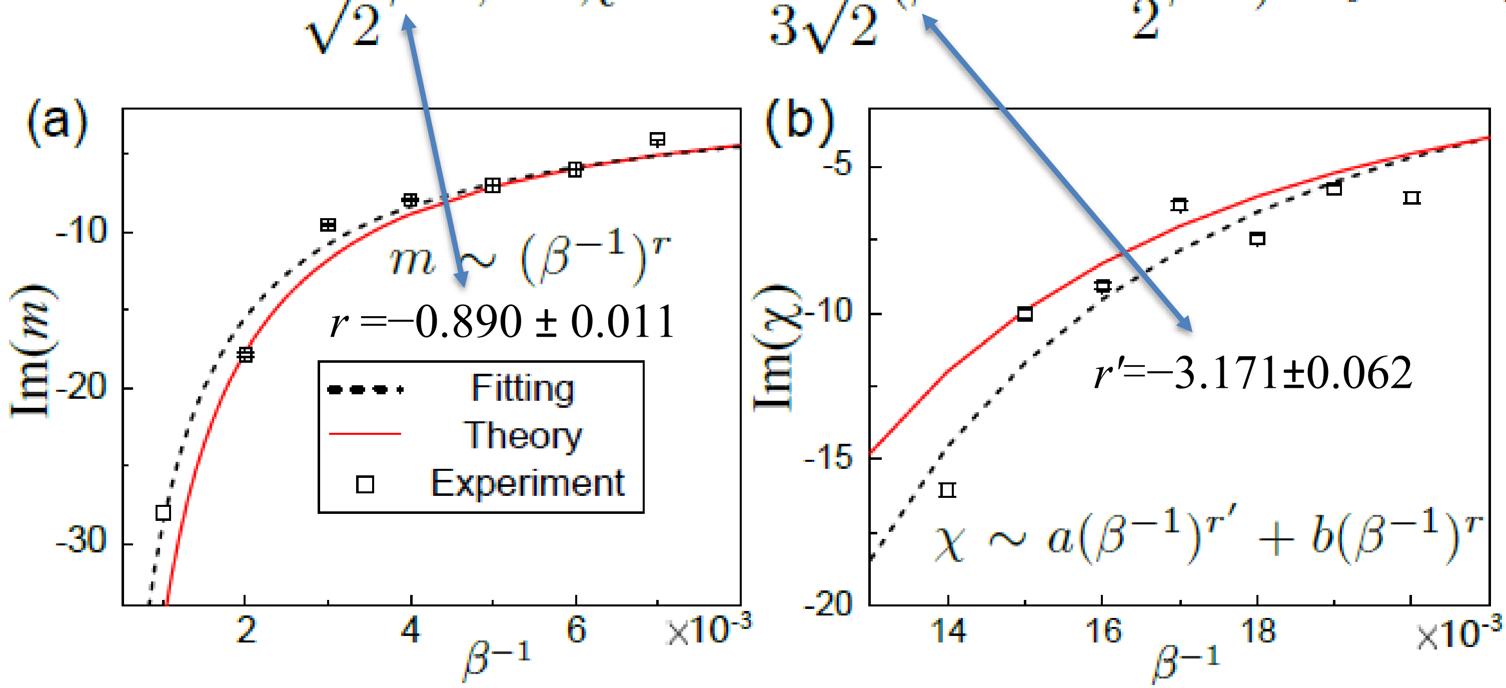

The measured results are consistent with theoretical predictions.

Direct observation of Yang-Lee zeros

H. Gao *et al.*, PRL **132**, 176601 (2024)

In the *PT*-broken phase, the measured partition function *Z* show periodic oscillations with period ~ 0.03 consistent with the theoretical prediction of π/100.

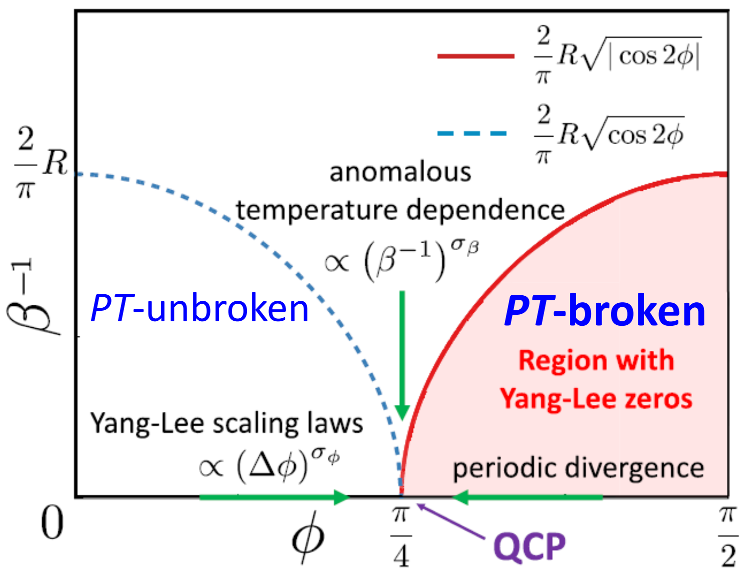

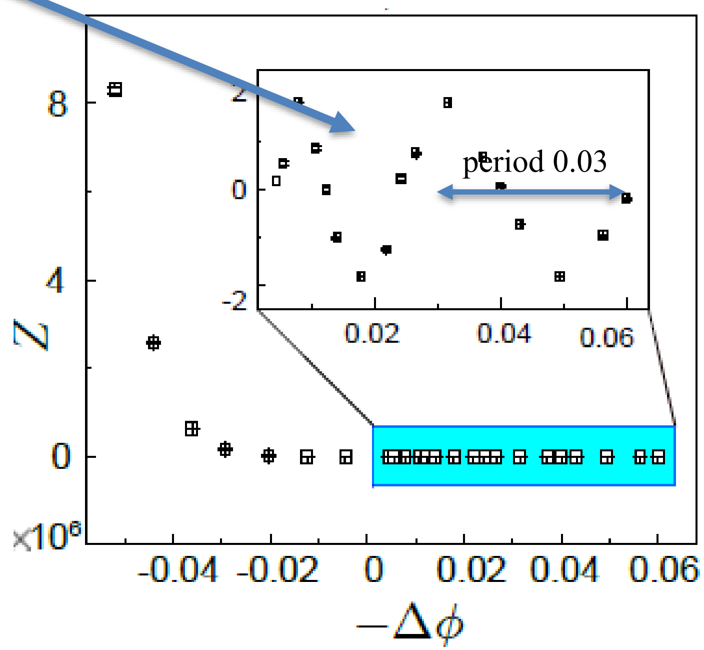

Observation of Yang-Lee edge singularity

H. Gao *et al.*, PRL **132**, 176601 (2024)

The measured density of Yang-Lee zeros $1/(\phi_{n+1}-\phi_n)$ show divergent behavior near the critical point π/4, which agrees with our prediction of the Yang-Lee edge singularity.

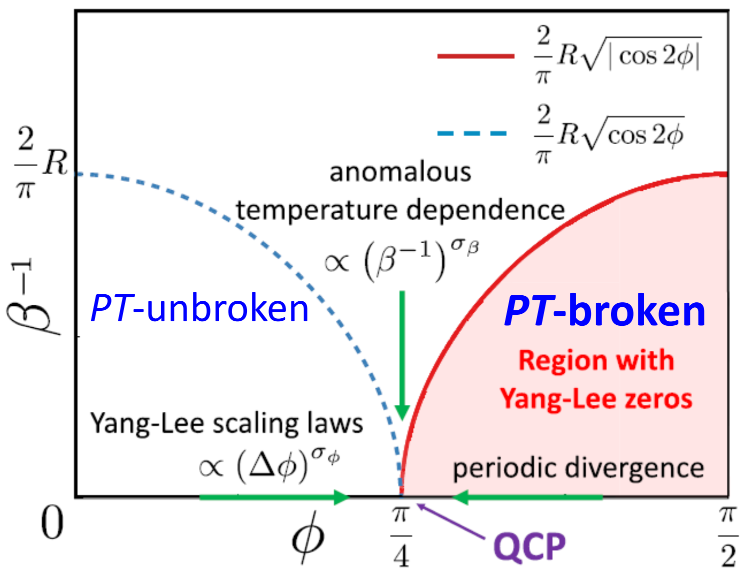

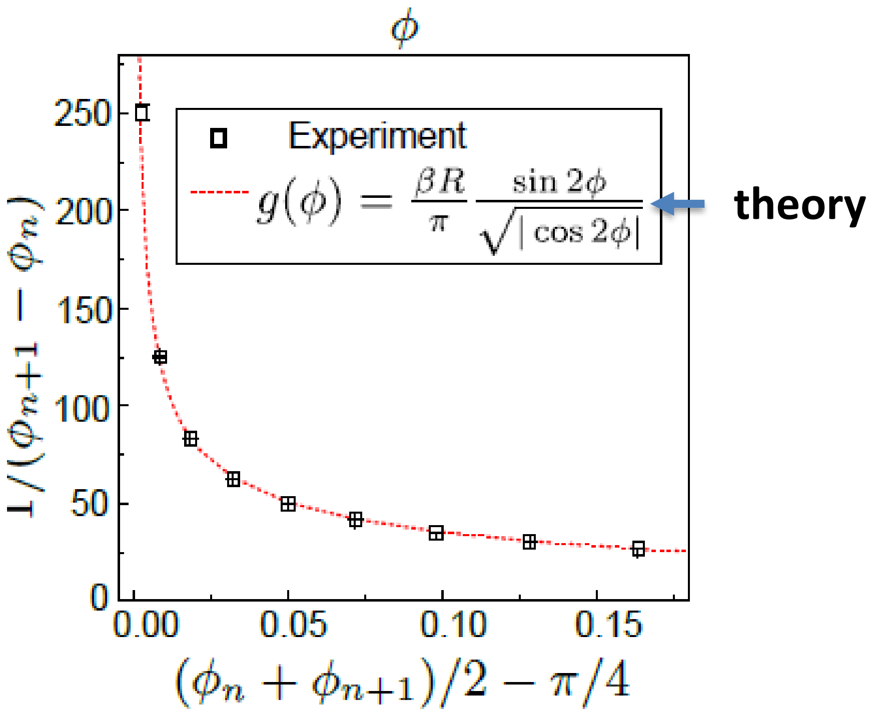

Observation of Yang-Lee edge singularity

H. Gao *et al.*, PRL **132**, 176601 (2024)

The measured density of Yang-Lee zeros 1/(ϕ_n … ϕ_n) show divergent behavior near the critical point π … h agrees with our prediction of the Yang-Lee ed… y.

A new quantum simulation paradigm for studying statistical physics!

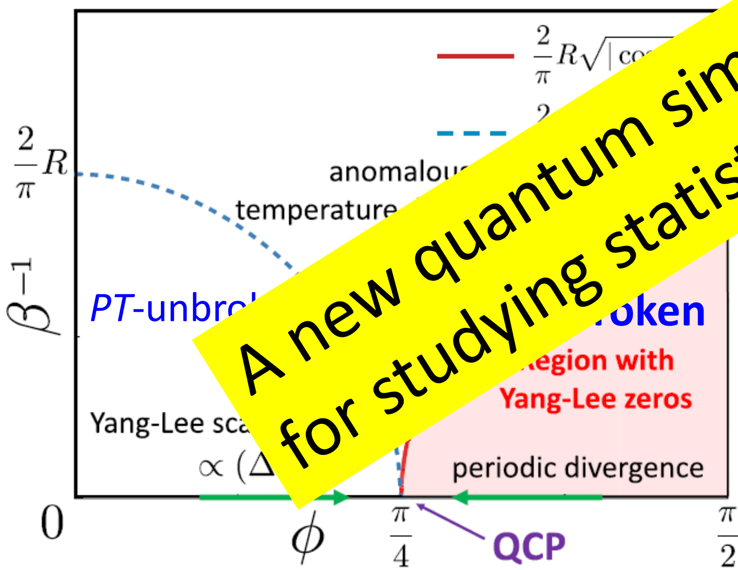

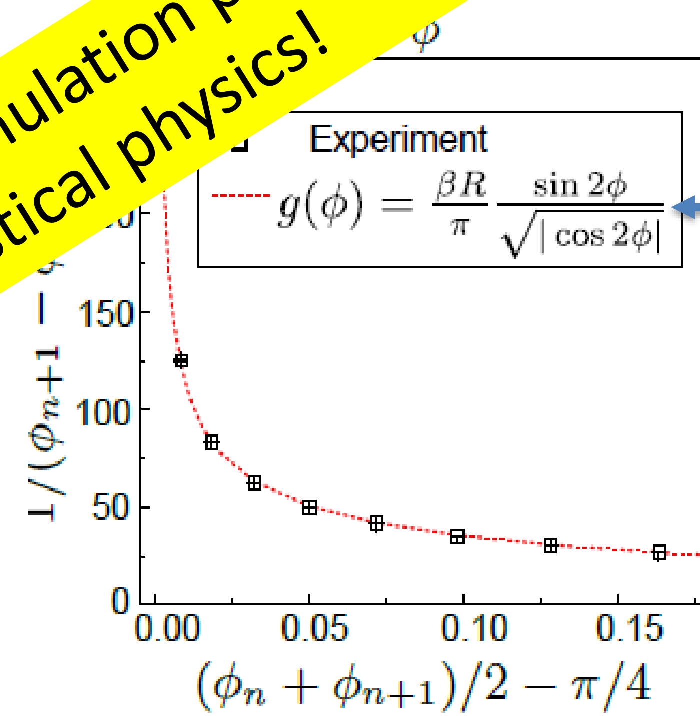

theory

Implications to condensed matter physics

Yang-Lee Zeros in BCS Superconductivity

H. Li, *et al*., Phys. Rev. Lett. **131**, 216001 (2023)

BCS Superfluidity with Complex Coupling

K. Yamamoto, *et al.*, Phys. Rev. Lett. **127**, 123601 (2019)

We consider a BCS model with a complex coupling constant *U*:

$$H = \sum_{k\sigma} \xi_k c^\dagger_{k\sigma} c_{k\sigma} - \frac{U}{N} \sum_{k,k'}{}' c^\dagger_{k\uparrow} c^\dagger_{-k\downarrow} c_{-k'\downarrow} c_{k'\uparrow} \qquad U = U_R + iU_I$$

The BEC wavefunction has the left and right components:

$$|\mathrm{BCS}\rangle_R = \prod_k (u_k + v_k c^\dagger_{k\uparrow} c^\dagger_{-k\downarrow})|0\rangle \qquad u_k^2 + v_k \bar{v}_k = 1$$

$$|\mathrm{BCS}\rangle_L = \prod_k (u_k^* + \bar{v}_k^* c^\dagger_{k\uparrow} c^\dagger_{-k\downarrow})|0\rangle$$

The Bogoliubov energy spectrum and the energy gap:

$$E_k = \sqrt{\xi_k^2 + \Delta_k^2} \qquad \Delta_k = \Delta_0 \theta(\omega_D - |\xi_k|)$$

$$\Delta_0 = \frac{\omega_D}{\sinh\left(\frac{1}{\rho_0 U}\right)}$$

Δ_0 is complex in general, so is E_k.

Distribution of Yang-Lee Zeros

H. Li, *et al.*, Phys. Rev. Lett. **131**, 216001 (2023)

$$Z = \prod_{k,\sigma} Z_k = \prod_{k,\sigma} (1 + e^{-\beta E_k})$$

occupation 0 1

The Semicircle Theorem

H. Li, *et al.*, Phys. Rev. Lett. **131**, 216001 (2023)

For the partition function to vanish,

$$Z = \prod_{k,\sigma} Z_k = \prod_{k,\sigma} (1 + e^{-\beta E_k}) = 0 \xrightarrow{e^{-\beta E_k} = -1} \begin{aligned} &\mathrm{Re}(E_k) = 0 \ \text{ and} \\ &\mathrm{Im}(\beta E_k) = (2n+1)\pi \end{aligned}$$

$$\boxed{(\rho_0 \pi U_R)^2 + (\rho_0 \pi U_I - 1)^2 = 1, \quad U_R > 0} \qquad U = U_R + iU_I$$

Yang-Lee zeros are distributed on a semicircle on the complex plane of the coupling constant in sharp contrast to the full circle theorem for the Ising model.

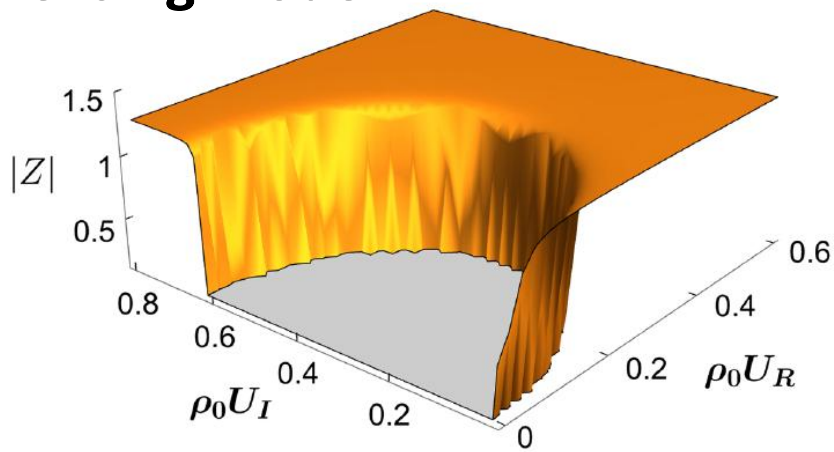

Why semicircle rather than full circle?

H. Li, *et al.*, Phys. Rev. Lett. **131**, 216001 (2023)

This is due to the attractive interaction ($U_R > 0$) needed for pairing instability.

$$\boxed{(\rho_0 \pi U_R)^2 + (\rho_0 \pi U_I - 1)^2 = 1, \quad U_R > 0} \qquad U = U_R + iU_I$$

Thus the semicircle arises from the Fermi-surface instability.

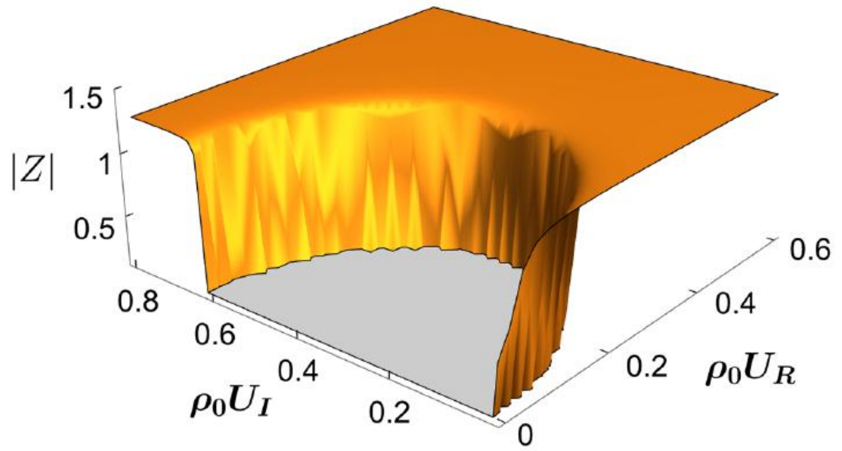

Physical Meaning of Yang-Lee zeros

H. Li, *et al*., Phys. Rev. Lett. **131**, 216001 (2023)

The number χ of Yang-Lee zeros is directly connected with Δ_0.

Yang-Lee zeros are determined by the conditions:

$$\mathrm{Re}(E_{\boldsymbol{k}}) = 0 \quad \text{and} \quad \mathrm{Im}(\beta E_{\boldsymbol{k}}) = (2n+1)\pi$$

Moreover,

$$\mathrm{Im}(\beta E_k) \in [0, \beta\, \mathrm{Im}(\Delta_0)].$$

$$\boxed{\chi \simeq \frac{\beta \mathrm{Im}(\Delta_0)}{\pi} = \frac{\beta \omega_D}{\pi \cosh\left(\frac{U_R}{\rho_0 |U|^2}\right)}}$$

Thus, the number of Yang-Lee zeros gives the SC energy gap.
Underlying physics has yet to be clarified.

Implications to cold atoms

Superfluidity without interactions

H. Li, *et al.*, PRL **135**, 166001 (2025)

- Bose-Einstein condensation and superfluidity are neither necessary and sufficient to each other.

- BEC of free bosons shows no superfluidity.

An ideal-gas BEC becomes a superfluid in the presence of two-body loss.

- **An ideal-gas BEC exhibits no superfluidity because the compressibility *κ***

$$\kappa = \frac{1}{Un^2}$$

diverges for *U*→0 (no interaction).

- **With two-body loss γ, the compressibility remains finite for *U*→0.**

$$\kappa = \frac{U_R}{(U_R^2 + \gamma^2)n^2} \longrightarrow$$

phase rigidity
superfluidity

Ideal-gas BEC under rotation

H. Li, *et al.*, PRL **135**, 166001 (2025)

$$(i-\gamma)\,\hbar\frac{\partial\Psi}{\partial t}=\left(-\frac{\hbar^2}{2m}\nabla^2-\mu+i\,g\,|\,\Psi\,|^{\,2}+\frac{1}{2}m\omega^2\,(\varepsilon_x x^2+\varepsilon_y y^2)-\Omega L_z\right)\Psi$$

***g*=0 without dissipation**

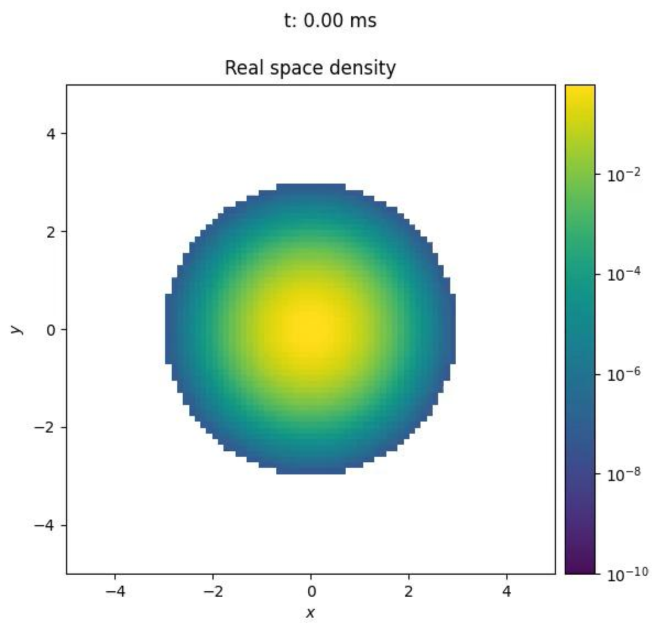

Ideal-gas BEC under rotation

H. Li, *et al.*, PRL **135**, 166001 (2025)

$$(i-\gamma)\,\hbar\frac{\partial\Psi}{\partial t}=\left(-\frac{\hbar^2}{2m}\nabla^2-\mu+i\,g\,|\,\Psi\,|^2+\frac{1}{2}m\omega^2(\varepsilon_x x^2+\varepsilon_y y^2)-\Omega L_z\right)\Psi$$

***g*=0 without dissipation**

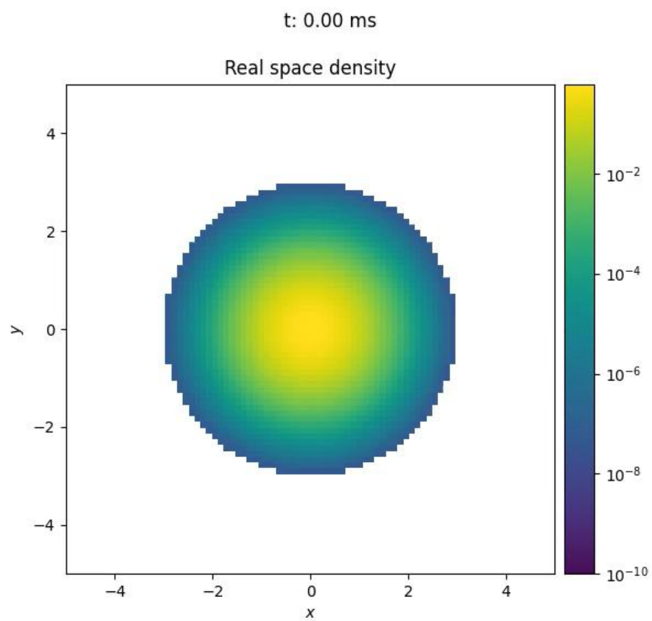

***g*≠0 with two-body loss**

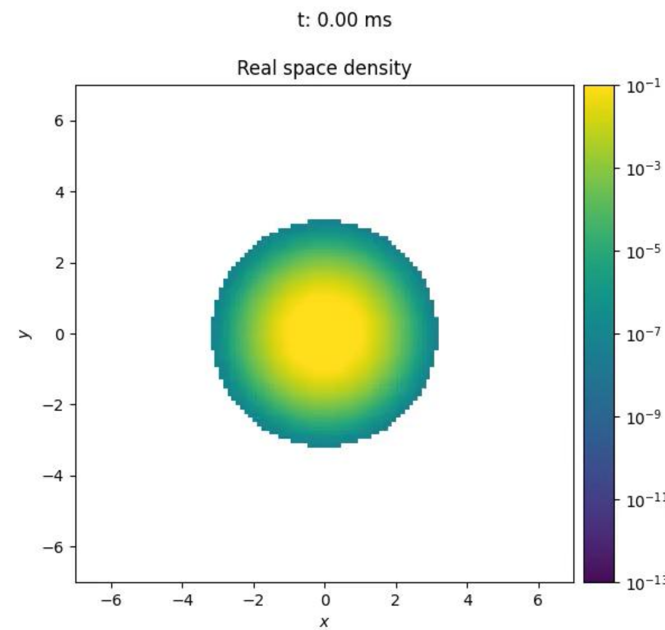

An ideal-gas BEC acquires superfluidity due to two-body loss.

Summary: toolbox of beyond-Hermitian physics

- **Nonunitary dynamics & *PT* symmetry**

  transport beyond LR bound PRL **120**, 185301 (2018)

  quantum criticality Nat. Commun. **8**, 15791 (2017)

- **Complex spectra** PRL **124**, 147203 (2020)

  intermediate-state engineering & magnetism reversal

- **Non-orthogonal eigenstates**

  continuous phase transitions without gap closing PRL **125**, 260601 (2020)

- **Yang-Lee zeros, nonunitary criticality, semicircle theorem**

  photonic quantum simulation PRL **132**, 176601 (2024)

  semicircle theorem in BCS superconductivity PRL **131**, 216001 (2023)

- **Extension of topological classification 10 → 38**

  PRX **8**, 031079 (2018); ibid. **9**, 041015 (2019)

- **Dissipation-induced superfluidity**

  PRL **135**, 166001 (2025)

These new phenomena exemplify only a tip of the iceberg of very rich beyond-Hermitian physics.

For a comprehensive review, Adv. Phys. **69**, 249 (2020)

Thank you very much!